

# Escape of $\alpha$ -particle in inertial confinement fusion

Kai Li<sup>1,\*</sup> and Ke Lan<sup>1,†</sup>

<sup>1</sup>*Institute of Applied Physics and Computational Mathematics, Beijing 100088, China*

(Dated: August 21, 2019)

Escape of  $\alpha$ -particles from a burning or an ignited burning deuterium-tritium (DT) fuel with temperature up to more than tens keV is very important in inertial confinement fusion, which can significantly influence not only the hot spot dynamics and the energy gain but also the shielding design in fusion devices. In this paper, we study the  $\alpha$ -particle escape from a burning or an ignited burning DT fuel by considering the modifications including the  $\alpha$ -particle stopping by both DT ions and electrons with their Maxwellian average stopping weights, the relativity effect on electron distribution, and the modified Coulomb logarithm of the DT- $\alpha$  particle collisions. As a result of our studies, the escape-effect from our modified model is obviously stronger than those from the traditional models. A fitted expression is presented to calculate the escape factor in a DT fuel, which can be applied to a burning fuel with temperatures of 1 to 150 keV and areal densities of 0.04 to 3 g/cm<sup>2</sup> with an accuracy within  $\pm 0.02$ . Finally, we discuss the  $\alpha$ -particle escape-effect on the hot-spot dynamics and the thermonuclear energy gain by comparing the results with escape factors from different models.

## I. INTRODUCTION

In Inertial Confinement Fusion (ICF) [1–3], a spherical encapsulated equimolar deuterium-tritium (DT) fuel is imploded isotropically either directly by lasers [4] or indirectly by X-ray radiation converted inside a hohlraum from lasers [5–8] to a very high velocity of about  $3 \times 10^7$  to  $4 \times 10^7$  cm/s, so that the fuel is highly compressed by rocket effect [9–11] to extreme density, temperature and pressure under the spherical convergent effect, and a hot spot with an areal density of about 0.3 g/cm<sup>2</sup> and a temperature of about 5 keV is formed in the center, triggering the nuclear fusion of the main fuel and resulting in a significant thermonuclear energy gain. Thermonuclear ignition and burn of a plasma occurs when self-heating by fusion products  $\alpha$ -particles exceeds all energy losses such that no further external heating is necessary to keep the plasma in the burning state. That is to say, the  $\alpha$ -particle self-heating is a prerequisite of ignition and burn of the fuel plasma. However, not all fusion produced  $\alpha$ -particles can be deposited in the fuel, because part of them can escape. Calculation of the escape of the  $\alpha$ -particles can significantly influence not only the theoretical studies on the ignition condition and the fusion energy gain but also the designs of the ignition targets. Especially, for an ignited burning fuel, its temperature can be up to more than tens keV, while the escape-effect is larger at a higher temperature and it can seriously influence the shielding material and configuration design of future fusion reactors.

Up to now, various theoretical models have been developed for the  $\alpha$ -particle escape, such as the Krokhin and Rozanov model [12] (KR model), the Fraley model [13], the Atzeni and Meyer-ter-Vehn [14] model (AM model), and the latest Zylstra and Hurricane model (ZH model) [15]. The first model to estimate the escape-effect of  $\alpha$ -particles was proposed by Krokhin and Rozanov [12] and then improved by Atzeni and Meyer-ter-Vehn [14], which are widely used till now [16–22]. In KR model, it ignored the deceleration of  $\alpha$ -particles

induced by DT ions and assumed a fuel with uniform density and temperature. As a result, the ratio of the escaped energy to the initial energy of the  $\alpha$ -particles, called as the escape factor of  $\alpha$ -particle in this paper, is obtained analytically as

$$\eta_A = \begin{cases} \frac{1}{4\tau} - \frac{1}{160\tau^3}, & \tau \geq \frac{1}{2} \\ 1 - \frac{3\tau}{2} + \frac{4}{5}\tau^2, & \tau < \frac{1}{2} \end{cases}, \quad (1)$$

for the spherical DT fuel. Here,  $\tau = \frac{\rho R}{\rho l_\alpha}$  is stopping depth of  $\alpha$ -particle in the fuel,  $\rho$  is density,  $\rho R$  is areal density of the fuel,  $l_\alpha$  is  $\alpha$ -particle range, and  $\rho l_\alpha$  is areal density range of the  $\alpha$ -particles. In AM model, it gives a fitted formula for  $\rho l_\alpha$  as

$$\rho l_\alpha = \frac{0.025T^{\frac{5}{4}}}{1 + 0.0082T^{\frac{5}{4}}} \quad (2)$$

by taking the DT ions into account, and uses Eq. (1) to calculate  $\eta_A$ . Here,  $\rho l_\alpha$  is in units of g/cm<sup>2</sup> and  $T$ , the temperature of the fuel, is in units of keV. According to a comparison among the KR model, the Fraley model and the AM model by Ref. [15], the AM model has the longest calculated range of the  $\alpha$ -particles and thus the lowest heating efficacy, which results from the calculation at densities more relevant to modern ICF designs in the AM model. In the latest ZH model, it used the modern stopping-power theories and gave an expression for calculating the  $\alpha$ -particle escape from a fuel of temperature limited in the range of 1~10 keV.

Notice that it uses Eq. (1) to calculate the  $\alpha$ -particle escape factor in AM model, which involves the  $\alpha$ -particle stopping induced only by electrons. Thus, it needs a consistent expression for the  $\alpha$ -particle escape factor, which considers the stopping contributions not only from electrons but also from the DT ions. In addition, the Coulomb logarithms for the DT- $\alpha$  collisions in AM model is obtained by using the thermal velocity of the DT ions as the relative velocity between these two kinds of particles, which needs to be modified when an  $\alpha$ -particle velocity is much higher than the thermal velocity of the DT ions. Furthermore, for an ignited burning fuel with temperatures up to tens to hundred keV, the relativity effect

\* likai@csrc.ac.cn

† ke\_lan@hotmail.com

on the electron velocity distribution can not be neglected in calculating the  $\alpha$ -particle escape.

In this paper, based on the classical two-body Coulomb collision model, we will give modifications on the  $\alpha$ -particle escape factor, including the  $\alpha$ -particle stopping by both DT ions and electrons with their Maxwellian average stopping weights, the electron stopping weight modified by the relativity effect, and the relative velocity effect on the Coulomb logarithm of DT- $\alpha$  particle collisions. In the modifications, we also consider the quantum effect on the Coulomb logarithm of DT- $\alpha$  particle collisions though it is small in the ICF range. As we know, the  $\alpha$ -particle escape factor is strongly connected with the time and space dependent plasma status of the fuel. However, to compare the escape factors from our model with those from the published models, we will consider a one-dimensional spherical DT fuel with uniform temperature and density and give a fitted expression of the  $\alpha$ -particle escape factor. Because the  $\alpha$ -particle escape can seriously influence the self-heating and the energy gain of a DT fuel, so we will further discuss and compare the  $\alpha$ -particle escape-effect on the hot-spot dynamics by using escape factors from different models.

This paper is organized as follows. In Sec. II, based on the classical two-body Coulomb collision model, we study the  $\alpha$ -particle escape from a DT fuel with temperatures up to more than tens keV by considering the Maxwellian averaged stopping weights of both DT ions and electrons, the electron stopping weight modified by the relativity effect, and the relative velocity effect and the quantum effect on Coulomb logarithm of the DT- $\alpha$  particle collisions. In Sec. III, we compare the  $\alpha$ -particle escape factor from our model with those from previous published models for a DT fuel. In Sec. IV, we study the escape-effect of the  $\alpha$ -particles on hot-spot dynamics of a DT fuel by using different escape factors. Finally, we will present a summary in Sec. V.

## II. STOPPING OF $\alpha$ -PARTICLE

In a burning fuel or an ignited burning fuel with strong self-heating, the temperature can range from a few keV to more than hundred keV. Inside such a fuel, the stopping of the 3.54 MeV  $\alpha$ -particle is mainly contributed by thermal electrons and thermal fuel ions via collisions, which is usually described by the Coulomb collision model. In this work, we take the two-body classical elastic Coulomb collisions for a fully ionized fuel and truncate the impact parameter at Debye shielding length [23]. The total energy loss within a path length  $ds$  of an  $\alpha$ -particle with an instantaneous energy  $E_\alpha$  is calculated as

$$\frac{dE_\alpha}{ds} = - \sum_j \left( \frac{dE_\alpha}{ds} \right)_j, \quad (3)$$

where the subscript  $j$  represents the particles of different species which collide with the  $\alpha$ -particles, and it refers to either thermal electrons or thermal DT ions for a fully ionized

pure DT plasma in the fuel. We have:

$$\left( \frac{dE_\alpha}{ds} \right)_j = \frac{n_j (q_\alpha q_j)^2 \ln \Lambda_j}{8\pi \mu_j \varepsilon_0^2 v_\alpha} \int_0^\infty f_j(v_j) h_j(v_j) dv_j, \quad (4)$$

where it is assumed that the species  $j$  has an isotropic velocity distribution function of  $f_j(v_j)$ . In Eq. (4),  $n$  is the number density,  $q$  is the charge,  $v$  is the velocity and the subscript refers to either a species  $j$  or an  $\alpha$ -particle,  $\varepsilon_0$  is the permittivity of vacuum,  $\ln \Lambda_j$  is the Coulomb logarithm of  $j$ - $\alpha$  collision, and  $\mu_j = \frac{m_\alpha m_j}{m_\alpha + m_j}$  is the reduced mass of a species  $j$  and an  $\alpha$ -particle, respectively. Notice that the factor  $h(v_j)$  weights the deceleration or acceleration of an  $\alpha$ -particle with  $v_\alpha$  when it collides with a  $j$ -particle with  $v_j$ , which is written as

$$h_j(v_j) = \begin{cases} -\frac{2\mu_j}{m_\alpha v_j}, & v_j > v_\alpha \\ \frac{2}{v_\alpha} \left( 1 - \frac{\mu_j}{m_\alpha} \right), & v_j \leq v_\alpha \end{cases}. \quad (5)$$

Thus, an  $\alpha$ -particle is decelerated by a slower  $j$ -particle with  $v_j < v_\alpha$ , while accelerated by a faster  $j$ -particle with  $v_j > v_\alpha$ . However, the deceleration weight can be different from the acceleration weight. From Eq. (5), the deceleration weights are remarkably higher than the acceleration weights for either DT ions or electrons. Especially, the deceleration weight of a slow electron can be at least four orders higher than the acceleration weight of a fast electron, as presented in Fig. 1. From Eq. (4), the  $\alpha$ -particle stopping is strongly connected with the  $\alpha$ -particle velocity, the velocity distribution of species  $j$  and the Coulomb logarithm of  $j$ - $\alpha$  collision. In the following, we consider following modifications on the  $\alpha$ -particle stopping inside an ignited burning fuel with fully ionized DT plasmas: the  $\alpha$ -particle stopping by both DT ions and electrons with their Maxwellian average stopping weights, the electron stopping weight modified by the relativity effect, and the modified Coulomb logarithm of the DT- $\alpha$  collisions with the relative velocity effect and the quantum effect, respectively.

### A. Maxwell-averaged stopping weights

Assuming the  $j$  species is in thermal equilibrium with the Maxwellian velocity distribution, we can obtain the same result as in Ref. [12] from Eq. (4):

$$\left( \frac{dE_\alpha}{ds} \right)_j = \frac{q_\alpha^2 q_j^2 n_j}{4\pi m_j \varepsilon_0^2 v_\alpha^2} \ln \Lambda_j g_j \left( \frac{v_\alpha}{v_{th,j}} \right). \quad (6)$$

Here,  $v_{th,j} = \sqrt{\frac{2T_j}{m_j}}$  is the thermal velocity of  $j$  species at its temperature  $T_j$ , and  $g_j$  is a function of the ratio of  $v_\alpha$  to  $v_{th,j}$  with the following expression:

$$g_j(x) = \text{erf}(x) - \left( 1 + \frac{m_j}{m_\alpha} \right) x \frac{d}{dx} \text{erf}(x), \quad (7)$$

where  $\text{erf}(x) = \frac{2}{\sqrt{\pi}} \int_0^x \exp(-y^2) dy$  is the error function. We call  $g_j$  as the stopping weight of  $j$  species on the  $\alpha$ -particle

energy change per unit length, which is important in calculating the escape of  $\alpha$ -particles.

We consider the  $\alpha$ -particle stopping inside a burning fuel or an ignited burning fuel of fully ionized DT plasmas. Transferring inside the DT fuel, an  $\alpha$ -particle with initial velocity  $v_\alpha^0$  collides with both DT ions and electrons, and its velocity varies and can be obviously lower than  $v_\alpha^0$ . We use  $g_{DT}$  and  $g_e$  to express the stopping weight of DT ions and electrons, respectively. For  $v_\alpha \ll v_{th,e}$ , which is always valid in the total deceleration process of  $\alpha$ -particle at  $T_e \gg 1$  keV,  $g_e$  can be written approximately as

$$g_e\left(\frac{v_\alpha}{v_{th,e}}\right) \approx \frac{4}{3\sqrt{\pi}}\left(\frac{v_\alpha}{v_{th,e}}\right)^3, \quad (8)$$

which is widely used in previous works [12, 13]. In the following text, we use this approximation for  $g_e$ .

If we neglect the slow variations of  $\ln \Lambda_{DT}$  and  $\ln \Lambda_e$ , then the ratio of the stopping contribution from DT ions to that from electrons is mainly decided by  $m_e g_{DT}/(m_{DT} g_e)$  from Eq. (6). To compare with  $g_{DT}$ , we define  $g_{e*} = \frac{m_{DT}}{m_e} g_e$ . Presented in Fig. 2 is the variations of  $g_{DT}$  and  $g_{e*}$  as  $v_\alpha/v_\alpha^0$  at  $T_{DT} = T_e = 100$  keV. As shown, the electron stopping weight is larger than the DT ion stopping weight for a newly produced  $\alpha$ -particle with a velocity around  $v_\alpha^0$ . However, the stopping weight of DT ions is obviously larger than that of the electrons during almost whole deceleration phase of an  $\alpha$ -particle, such as with its velocity decreasing from  $0.95v_\alpha^0$  to  $0.2v_\alpha^0$  at 100 keV. With a velocity of about  $0.2v_\alpha^0$ , the same as  $v_{th,DT}$  at 100 keV, the  $\alpha$ -particle stops deceleration at this temperature. In the following, we discuss the stopping of  $\alpha$ -particle by the DT ions and the electrons, respectively.

From Fig. 2,  $g_{DT}$  at 100 keV approaches its maximum of 1 at  $v_\alpha > 0.5v_\alpha^0$ , but it drops abruptly as decrease of  $v_\alpha$  at  $v_\alpha \lesssim 0.5v_\alpha^0$  and even drops to zero at  $v_\alpha = 0.2v_\alpha^0$ . In particular,  $g_{DT}$  is negative at  $v_\alpha < 0.2v_\alpha^0$  from Fig. 2 or at  $v_\alpha < 0.84v_{th,DT}$  from Eq. (7), which means that an  $\alpha$ -particle with a velocity lower than  $v_{th,DT}$  can even gain energy from DT ions instead of losing energy to DT ions in this case. Thus, the stopping condition of  $\alpha$ -particle should be defined as  $v_\alpha = v_{th,DT}$ , instead of  $v_\alpha = 0$ . Here, it is worth to mention that an approximation of  $g_{DT} \approx 1$  is often used in previous works [12–14] with a consideration of  $v_{th,DT} \ll v_\alpha$ , which seriously overestimates the  $\alpha$ -particle stopping power by using a much bigger stopping weight of 1 for those  $\alpha$ -particles with velocities obviously lower than  $v_\alpha^0$ .

Again from Fig. 2,  $g_{e*}$  at 100 keV is obviously larger than  $g_{DT}$  at  $v_\alpha > 0.95v_\alpha^0$ , while much smaller than  $g_{DT}$  at  $0.2v_\alpha^0 \leq v_\alpha \leq 0.95v_\alpha^0$ . It means that the stopping is mainly dominated by the electrons for the newborn  $\alpha$ -particles or when the  $\alpha$ -particles are in the initial status of deceleration, while dominated by the DT ions after the  $\alpha$ -particle is significantly decelerated. Thus, calculation of  $g_e$  is especially important for a newborn  $\alpha$ -particle. In addition,  $g_{e*}$  is about zero at  $v_\alpha < 0.2v_\alpha^0$  at 100 keV from Fig. 2, which means the electrons have no influence at all for those seriously decelerated  $\alpha$ -particles.

## B. Electron stopping weight modified by relativity effect

As shown in Fig. 1, the stopping of the  $\alpha$ -particles by electrons is dominated by the slow electrons which velocities satisfy  $v_e \leq v_\alpha \ll c$ , where  $c$  is the velocity of light in vacuum. It means that the dynamics of Coulomb collision between  $\alpha$ -particles and electrons exempt from the relativity effect, but nevertheless, the number of electrons with velocities  $v_e \leq v_\alpha$  is very different when the relativity effect is taken into account at a temperature higher than tens keV, which is easily achieved in an ignited burning fuel. Thus, the relativity can influence the stopping via the electron distribution. Here, we consider the relativity effect and give a modification on the electron stopping weight  $g_e$ .

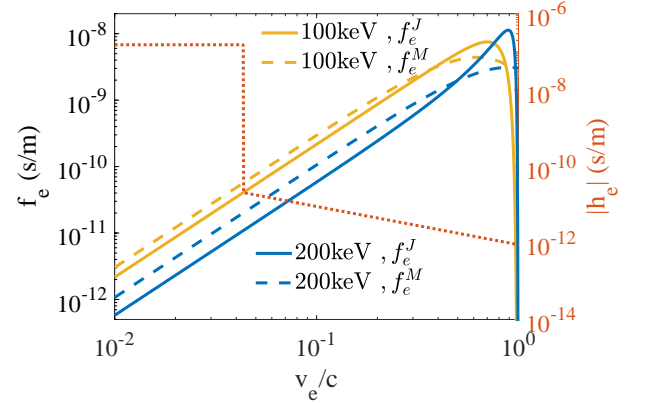


FIG. 1. (Color online) Absolute value of  $h_e(v_e)$  from Eq.(5) (dotted red, right y-axis) and comparisons (left y-axis) between the Maxwell distributions (dashed lines) and the Maxwell-Jüttner distributions (solid lines) for electrons at 100 keV (yellow) and 200 keV (blue).

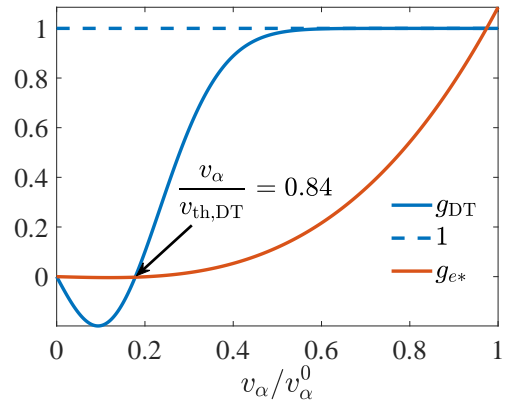


FIG. 2. (Color online) Variations of  $g_{DT}$  (full blue),  $g_{e*}$  (full red) as  $v_\alpha/v_\alpha^0$  at  $T_{DT} = T_e = 100$  keV. The approximation of taking  $g_{DT} = 1$  (dashed blue) is also given for comparison.

In deducing Eq. (6) from Eq. (4), we use the following Maxwell distribution function of electrons without consider-

ing the relativity effect:

$$f_e^M(v_e) = \frac{4}{\sqrt{\pi}} v_{\text{th},e}^{-3} v_e^2 \exp\left(-\frac{v_e^2}{v_{\text{th},e}^2}\right). \quad (9)$$

However, the electron velocity follows the Maxwell-Jüttner distribution function when the relativity effect is taken into consideration [24]:

$$f_e^J(v_e) = \frac{v_e^2}{\gamma c^3 K_2(\frac{1}{\gamma})} \lambda^5 \exp\left(-\frac{\lambda}{\gamma}\right). \quad (10)$$

Here  $\gamma = \frac{T_e}{m_e c^2}$ ,  $\lambda = (1 - \frac{v_e^2}{c^2})^{-\frac{1}{2}}$ , and  $K_2$  is the second order modified Bessel function [25]. As shown in Fig. 1, it has a significant difference between the Maxwell distribution and the Maxwell-Jüttner distribution for the slow electrons at 100 keV and 200 keV. At a higher temperature, the difference between the two kinds of electron velocity distributions is bigger. We can define a relativity factor  $\xi$  as:

$$\xi = \frac{\int_0^c f_e^J(v_e) h_e(v_e) dv_e}{\int_0^c f_e^M(v_e) h_e(v_e) dv_e}, \quad (11)$$

and modify the electron stopping weight  $g_e$  as  $\xi g_e$  under the relativity effect. Considering that the stopping weight of electrons is mainly contributed by the slow electrons with velocity of  $v_e \leq v_\alpha \ll \{v_{\text{th},e}, c\}$ , we can take an expansion of the two distribution functions Eqs. (9, 10) at  $v_e = 0$ , respectively, as

$$f_e^M(v_e) \approx \frac{4}{\sqrt{\pi}} v_{\text{th},e}^{-3} v_e^2, \quad (12)$$

$$f_e^J(v_e) \approx \frac{v_e^2}{\gamma c^3 K_2(\frac{1}{\gamma})} \exp(-\frac{1}{\gamma}). \quad (13)$$

Further considering that function  $h_e(v_e)$  has a constant value in the interval  $v_e \leq v_\alpha$  from Eq. (5), we have

$$\xi \approx \frac{\sqrt{\pi} v_{\text{th},e}^3 \exp(-\frac{1}{\gamma})}{4\gamma c^3 K_2(\frac{1}{\gamma})}. \quad (14)$$

In addition, we also take an expansion of  $K_2(\frac{1}{\gamma})$  at  $\gamma = 0$  by considering  $\gamma \ll 1$  at  $T_e \ll m_e c^2 \approx 511$  keV. Then the relativity factor can be simplified as

$$\begin{aligned} \xi &\approx \frac{\sqrt{2} v_{\text{th},e}^3}{4c^3 (\gamma^{\frac{3}{2}} + \frac{15}{8} \gamma^{\frac{5}{2}})} \\ &= \frac{8}{8 + 15\gamma}. \end{aligned} \quad (15)$$

Notice that Eq. (15) depends only on  $T_e$ . At a very low  $T_e$  with  $\gamma \approx 0$ ,  $\xi$  tends to 1, and the Maxwell-Jüttner distribution approaches the Maxwell distribution. As  $T_e$  increases, the number of electrons with  $v_e < v_\alpha$  decreases under both distributions, but this effect is more significant under the Maxwell-Jüttner distribution, as shown in Fig. 1. It means that the electron stopping weight decreases more seriously as  $T_e$  increases under the Maxwell-Jüttner distribution. In other words, the relativity effect of the electrons increases the escape probability of the  $\alpha$ -particles out of fuel. For example,  $\xi \approx 0.73$  at  $\gamma \approx 0.2$  or  $T_e = 100$  keV, which means that relativity effect leads to a decrease of 27% on the electron stopping weight as compared to the result under the Maxwell distribution.

### C. Modifications on Coulomb logarithms

From Eq. (6), the  $\alpha$ -particle stopping is connected with  $\ln \Lambda_{\text{DT}}$  and  $\ln \Lambda_e$ , which are the Coulomb logarithms for collisions between the  $\alpha$ -particles and the DT ions and collisions between the  $\alpha$ -particles and the electrons, respectively. Generally, the Coulomb logarithm is calculated with

$$\ln \Lambda_j = \ln \frac{\lambda_D}{\max(l_{j,C}, l_{j,Q})}, \quad (16)$$

where

$$\lambda_D = \sqrt{\frac{\varepsilon_0 T}{2e^2 n}} \quad (17)$$

is the Debye shielding length,  $l_{j,C}$  is a velocity-averaged classical impact parameter, and  $l_{j,Q}$  is a velocity-averaged quantum impact parameter. Here, we assume  $T_e = T_{\text{DT}} \equiv T$ ,  $n_e = n_{\text{DT}} \equiv n$ , and the factor 2 in Eq. (17) accounts for the Debye shielding induced by both electrons and DT ions. The classical impact parameter for a  $90^\circ$  scattering of  $j$ - $\alpha$  collision is

$$l_{j,C} = \frac{q_\alpha q_j}{4\pi \varepsilon_0 \mu_j u_j^2} \quad (18)$$

with  $u_j = |\mathbf{v}_\alpha - \mathbf{v}_j|$  the relative velocity between  $j$  and  $\alpha$ -particle, and the quantum impact parameter is  $l_{j,Q} = \lambda_q / 4\pi$  with  $\lambda_q = 2\pi \hbar / \mu_j u_j$  the de Broglie wavelength [26]. For the plasma status interested for inertial fusion,  $e$ - $\alpha$  collisions are in quantum domain and the corresponding Coulomb logarithm can be found from Ref. [14]:

$$\ln \Lambda_e = 7.1 - 0.5 \ln n + \ln T \quad (19)$$

with  $n$  in units of  $10^{21}/\text{cm}^3$  and  $T$  in units of keV. However, DT- $\alpha$  collisions is a little complicated, which can be treated either as classical or as quantum, depending on the  $\alpha$  particle energy and the DT ion temperature, while it is seldom discussed in previous publications. Here, we take the Maxwell distribution for DT ions and obtain the average impact parameters for the DT- $\alpha$  collisions in both classical and quantum cases. We first define a  $T$ -dependent critical energy  $E_c$  to separate the classical domain from the quantum domain in calculating the Coulomb logarithm for the DT ions, which is fitted as:

$$E_c = 1663 - \frac{6.9T}{1 + 0.001T}, \quad (20)$$

where  $E_c$  and  $T$  are in units of keV. Then, with the Maxwell-averaged  $u_{\text{DT}}^2 = v_\alpha^2 + \frac{3}{2} v_{\text{th,DT}}^2$  and according to Eq. (16, 17, 18), the Coulomb logarithm with quantum effect for the DT- $\alpha$  collision can be given as:

$$\ln \Lambda_{\text{DT}} = \begin{cases} \ln \Lambda_{\text{DT,C}}, & E_\alpha < E_c \\ \ln \Lambda_{\text{DT,Q}}, & E_\alpha \geq E_c \end{cases}, \quad (21)$$

where  $\ln \Lambda_{\text{DT,C}}$  and  $\ln \Lambda_{\text{DT,Q}}$  are:

$$\ln \Lambda_{\text{DT,C}} = 7.25 + \ln(E_\alpha + 2.4T) + 0.5 \ln \frac{T}{n}, \quad (22)$$

$$\ln \Lambda_{\text{DT,Q}} = 10.94 + 0.5 \ln \frac{E_\alpha T}{n}. \quad (23)$$

Here,  $E_\alpha$  and  $T$  are in units of keV, and  $n$  is in units of  $10^{21}/\text{cm}^3$ . Nevertheless, the quantum effect on the Coulomb logarithm for the DT- $\alpha$  collision is very small, within 3%, in the range interested for ICF study.

In the AM model [14, 26], the Coulomb logarithms for DT- $\alpha$  collisions is written as

$$\ln \Lambda_{\text{DT},A} = 9.2 - 0.5 \ln n + 1.5 \ln T, \quad (24)$$

which is obtained by taking  $\frac{1}{2}\mu_{\text{DT}}u_{\text{DT}}^2 = \frac{3}{2}T$  with an assumption that the relative velocity between these two kinds of particles is the same as the thermal velocity of the DT ions. However, this assumption needs to be modified at  $v_\alpha \gg v_{\text{th,DT}}$ , especially for the newborn  $\alpha$ -particles.

In Fig. 3, we present the ratio of  $\ln \Lambda_{\text{DT}}$  to  $\ln \Lambda_{\text{DT},A}$  in the map of  $T$  and  $v_\alpha$ . As indicated, for  $\alpha$ -particles with  $v_\alpha \gg v_{\text{th,DT}}$  at 5 to 40 keV,  $\ln \Lambda_{\text{DT}}$  can be up to 1.6 times larger than  $\ln \Lambda_{\text{DT},A}$ . As we know, a larger Coulomb logarithms can lead to a stronger deposition of  $\alpha$ -particles and a weaker escape. Nevertheless, with all modifications considered in our model, the  $\alpha$ -particle escape from our model is still stronger than that from the AM model, as will be shown below.

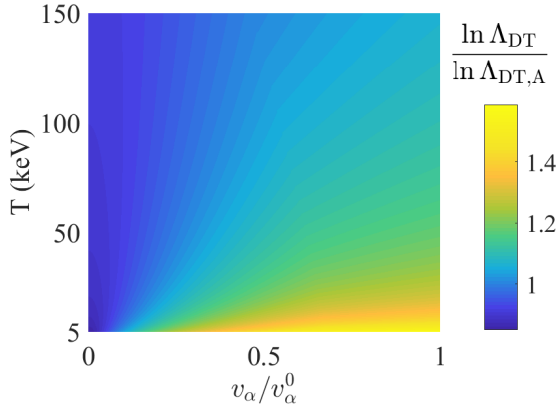


FIG. 3. (Color online) Color map of  $\ln \Lambda_{\text{DT}}$  to  $\ln \Lambda_{\text{DT},A}$  ratio as a function of  $E_\alpha$  and  $T_{\text{DT}} = T_e \equiv T$  from Eqs. (21, 24).

As a summary, we have considered the modifications of the  $\alpha$ -particle stopping by the DT ions and the electrons inside a fuel plasma with the Maxwellian average stopping weights, the relativity effect on electron stopping weight and the modified Coulomb logarithm of the DT- $\alpha$  particle collisions. Thus, the variation of  $\alpha$ -particle energy within a displacement  $ds$  inside a fully ionized DT plasma can be rewritten from Eqs. (3) and (6):

$$\frac{dE_\alpha}{ds} = \left(\frac{dE_\alpha}{ds}\right)_{\text{DT}} + \left(\frac{dE_\alpha}{ds}\right)_e \quad (25)$$

with

$$\left(\frac{dE_\alpha}{ds}\right)_{\text{DT}} = -\frac{m_\alpha}{m_{\text{DT}}} \frac{e^4}{2\pi\epsilon_0^2} \frac{n}{E_\alpha} \ln \Lambda_{\text{DT}} g_{\text{DT}}, \quad (26)$$

and

$$\left(\frac{dE_\alpha}{ds}\right)_e = -\frac{m_\alpha}{m_{\text{DT}}} \frac{e^4}{2\pi\epsilon_0^2} \frac{n}{E_\alpha} \xi \ln \Lambda_e g_{e*}. \quad (27)$$

Here, we take  $n_{\text{DT}} = n_e \equiv n$  for a fully ionized ignited burning DT fuel, with  $g_{\text{DT}}$  and  $g_{e*}$  calculated by using Eq. (7, 8), relativity factor  $\xi$  calculated by using Eq. (15), and the Coulomb logarithms  $\ln \Lambda_{\text{DT}}$  and  $\ln \Lambda_e$  calculated by using Eq. (19) and Eq. (22), respectively. It shows a nonlinear deceleration of  $\alpha$ -particles from Eq. (25), because it depends on  $E_\alpha$ ,  $n$ ,  $\ln \Lambda_{\text{DT}}$ ,  $\ln \Lambda_e$ ,  $\xi$ ,  $g_{\text{DT}}$  and  $g_{e*}$ , while these parameters are strongly time and space dependent inside a burning fuel plasma.

Here, it is interesting to compare the stopping contributions between the DT ions and the electrons. Taking the same temperature for the DT ions and the electrons,  $T_{\text{DT}} = T_e \equiv T$ , we obtain a map of  $\left(\frac{dE_\alpha}{ds}\right)_{\text{DT}}$  to  $\left(\frac{dE_\alpha}{ds}\right)_e$  ratio from Eq. (25), as presented in Fig. 4. As indicated, it has two critical lines for the  $\alpha$ -particles. One is between the DT ion dominated deceleration phase and the electron dominated deceleration phase, defined as  $\left(\frac{dE_\alpha}{ds}\right)_{\text{DT}} = \left(\frac{dE_\alpha}{ds}\right)_e$ . Another one is between the deceleration phase and the stopping phase, defined as  $v_\alpha = v_{\text{th,DT}}$ . The deceleration is mainly induced by the electrons for a newborn  $\alpha$ -particle at  $T \lesssim 50$  keV. At a lower  $T$ , it has more slow electrons, and the stopping from electron can dominate till to the case when the  $\alpha$ -particles are seriously decreased. At  $T > 50$  keV, the deceleration of the  $\alpha$ -particles is fully dominated by the DT ions, because it has very few electrons with velocity  $v_e \leq v_\alpha$ . For  $T > 5$  keV, as shown on the map, the deceleration phase of an  $\alpha$ -particle is dominated by the DT ions when the  $\alpha$ -particle is remarkably decelerated. At a higher  $T$ , it has a higher  $v_{\text{th,DT}}$ , thus an  $\alpha$ -particle stops deceleration and enters into its stopping phase with a higher velocity.

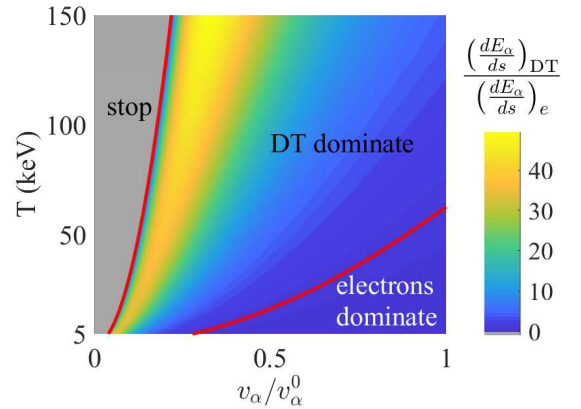


FIG. 4. (Color online) Color map of  $\left(\frac{dE_\alpha}{ds}\right)_{\text{DT}}$  to  $\left(\frac{dE_\alpha}{ds}\right)_e$  ratio in the plane of  $T$  and  $v_\alpha/v_{\alpha 0}$ , with the left red line representing  $\left(\frac{dE_\alpha}{ds}\right)_{\text{DT}} = 0$  when the  $\alpha$ -particle stops and the right red line representing  $\left(\frac{dE_\alpha}{ds}\right)_{\text{DT}} = \left(\frac{dE_\alpha}{ds}\right)_e$  when the DT ions and the electrons contribute the same on stopping the  $\alpha$ -particles. In the middle part with  $\left(\frac{dE_\alpha}{ds}\right)_{\text{DT}} > \left(\frac{dE_\alpha}{ds}\right)_e$ , the  $\alpha$ -particle stopping is dominated by the DT ions. In the right part with  $\left(\frac{dE_\alpha}{ds}\right)_{\text{DT}} < \left(\frac{dE_\alpha}{ds}\right)_e$ , the  $\alpha$ -particle stopping is dominated by the electrons.

### III. ESCAPE FACTOR OF $\alpha$ -PARTICLE

Escape of the  $\alpha$ -particles from a burning fuel is very important, which can seriously decrease the temperature of hot spot and thus fusion gain, and in addition, it can greatly influence a container design for future energy usage of inertial fusion.

$$\eta_E = \frac{1}{4\pi V E_\alpha^0} \int_V d\mathbf{r} \int_0^{2\pi} d\varphi \int_0^\pi d\theta E_{\text{esc}}(\mathbf{r}, \theta, \varphi) \sin \theta. \quad (28)$$

Here,  $V$  is the volume of the fuel ball, and the escaped energy for an  $\alpha$ -particle produced at  $\mathbf{r}$  with a launching angle  $(\theta, \varphi)$ , as shown in Fig. 5, is

$$E_{\text{esc}}(\mathbf{r}, \theta, \varphi) = \begin{cases} 0, & \text{if } \exists s \leq s_0, E_\alpha(s) \leq T_{\text{DT}} \\ E_\alpha(s_0), & \text{if } E_\alpha(s_0) > T_{\text{DT}} \end{cases}, \quad (29)$$

where  $s_0$  is the distance from point  $\mathbf{r}$  to the fuel surface along direction  $(\theta, \varphi)$ , and the remained energy of this  $\alpha$ -particle after transferring within a length of  $s$  is

$$E_\alpha(s) = \int_s \frac{dE_\alpha(s')}{ds'} ds'. \quad (30)$$

Here, the integration path is

$$\mathbf{s} = \mathbf{r} + s' \mathbf{k}(\theta, \varphi) \text{ with } 0 \leq s' \leq s, \quad (31)$$

where  $\mathbf{k}(\theta, \varphi)$  is the unit vector in the direction  $(\theta, \varphi)$ .

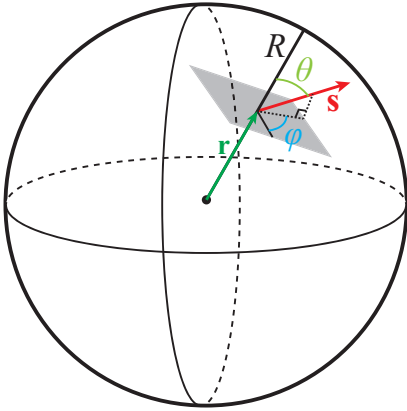


FIG. 5. (Color online) Diagram of  $\alpha$ -particles transferring inside a spherical DT fuel of radius  $R$ . An  $\alpha$ -particle produced at  $\mathbf{r}$  with a launching angle of  $(\theta, \varphi)$  transfers along the red path  $\mathbf{s}$ . Here,  $\theta$  is the angle between  $\mathbf{r}$  and  $\mathbf{s}$ , and  $\varphi$  is an azimuthal angle. The distance from  $\mathbf{r}$  to the surface of the ball along direction  $(\theta, \varphi)$  is  $s_0(r, \theta) = \sqrt{R^2 - r^2 \sin^2 \theta} - r \cos \theta$ , which is independent of  $\varphi$ .

The integration Eq. (30) is taken along the transferring trajectories  $\mathbf{s}$  of all  $\alpha$ -particles by considering the variations of temperature and density which are time and space dependent,

From Eq. (25), by assuming that the launching of  $\alpha$ -particles is isotropic and the  $\alpha$ -particles do not change their moving directions, same as in previous works [12, 14], we can define an escape factor of the  $\alpha$ -particles escaping from a spherical fuel plasma with radius of  $R$ :

as in Fig. 5. As presented in Eq. (29), we consider that an  $\alpha$ -particle is fully stopped in the DT plasma if the energy of this  $\alpha$ -particle reduces to  $T_{\text{DT}}$  at  $s \leq s_0$ , and in this case no energy of this  $\alpha$ -particle escaped. Or else, the remained energy  $E_\alpha(s_0)$  of this  $\alpha$ -particle will be carried out and lost from the DT fuel.

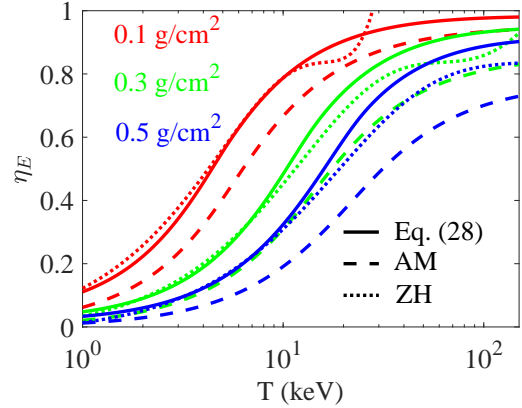


FIG. 6. (Color online) Comparisons among  $\eta_E$  from Eq. (28) (solid line), the AM model (dashed line) and the ZH model (dotted line) for a burning fuel with  $T$  varying from 1 to 100 keV at  $\rho R = 0.1$  g/cm<sup>2</sup> (red), 0.3 g/cm<sup>2</sup> (green) and 0.5 g/cm<sup>2</sup> (blue).

In what follows, we calculate  $\eta_E$  for a spherical DT fuel with uniform temperature and density, and compare  $\eta_E$  obtained by using different models, for the parameters, radius  $R = 50 \mu\text{m}$ ,  $\rho R = 0.1, 0.3, 0.5$  g/cm<sup>2</sup> and  $T = 1 \sim 100$  keV. Presented in Fig. 6 is comparisons among  $\eta_E$  obtained from Eq. (28), the AM model and the ZH model. As shown,  $\eta_E$  from the ZH model agrees well with that from Eq. (28) at  $T < 10$  keV, but it deviates from  $\eta_E$  from Eq. (28) at  $T > 10$  keV, for the reason that the expression of  $\eta_E$  in the ZH model is fitted in the range of 1~10 keV [15]. Notice that the AM model gives the lowest  $\eta_E$  as compared to the results from Eq. (28) and the ZH model, even at  $T \lesssim 5$  keV. The reason is that, the AM model calculates the escape factor with Eq. (1) from the KR model which ignores the deceleration of the  $\alpha$ -particles induced by the DT ions, though it calculate the  $\alpha$ -particle range with Eq. (2) which takes both DT ions and electrons into consideration. Thus, AM model gives a lower escape factor than from Eq. (28). This effect can be more re-

markable at a higher temperature, when the DT ions dominate the stopping more significantly and the relative effect is more seriously.

With all modifications of the  $\alpha$ -particle stopping by both

$$\eta_E = \frac{0.00593(\rho R)^{-1.174}T^{1.556}}{1 + 0.00385(\rho R)^{0.600}T^{1.316} + 0.00547(\rho R)^{-1.180}T^{1.574}}, \quad (32)$$

which can be applied to a burning fuel with temperatures ranging from 1~150 keV and areal density ranging from 0.04~3 g/cm<sup>2</sup> with an accuracy within  $\pm 0.02$ .

#### IV. ESCAPE-EFFECT ON HOT-SPOT DYNAMICS

In this section, we study the  $\alpha$ -particle escape effect on the hot-spot dynamics of an expanding burning plasma by supposing a DT fuel plasma which is an ideal gas composed with the DT ions and electrons with time-dependent uniform temperature and density for simplicity. To focus on the escape effect, we ignore the energy lost by radiation and by thermal conduction and only consider the self-heating by the fusion products  $\alpha$ -particles and the energy lost by expansion cooling via mechanical work. Thus, the dynamic equations of the hot-spot can be written as

$$\frac{dT}{dt} = \frac{2\pi}{9N}R^3 E_\alpha^0 n^2 \langle \sigma v \rangle (1 - \eta_E) - \frac{2T}{R} \frac{dR}{dt}, \quad (33)$$

$$\frac{dN}{dt} = -\frac{4\pi}{3}R^3 n^2 \langle \sigma v \rangle, \quad (34)$$

$$\frac{d^2R}{dt^2} = \frac{3NT}{m_s R}. \quad (35)$$

Here,  $N$  represents the total number of both DT ions and electrons. On the right-hand side of Eq. (33), the first term represents the self-heating induced by  $\alpha$ -particles with escape effect considered, and the second term represent the expansion cooling of a burning plasma due to its mechanical work. Eq. (34) describes the number change of the DT ions and electrons during the nuclear reaction, where we simply consider four particles are consumed in one reaction, including two DT ions burned and two electrons lost for electric neutrality. Eq. (35) describes the expansion dynamics of the burning hot-spot like that an ideal gas pushes a spherical piston outward with an acceleration of  $3NT/m_s R$ , where  $m_s$  is the effective mass of the piston. The reactivity of DT  $\langle \sigma v \rangle$  is [27]

$$\langle \sigma v \rangle = 9.1 \times 10^{-22} \exp\left(-0.572 \left| \ln \frac{T}{64.2} \right|^{2.13}\right), \quad (36)$$

where  $\langle \sigma v \rangle$  is in unit of m<sup>3</sup>/s and  $T$  is in unit of keV. The gain of the hot-spot can be defined as

$$G_H = \left(\frac{\Delta N}{4} E_{\text{fus}}\right) / \left(\frac{3}{2} T_0 N_0\right). \quad (37)$$

DT ions and electrons with their Maxwellian average stopping weights, the relativity effect on electron distribution and the modified Coulomb logarithm of DT- collisions, we have a fitted expression of  $\eta_E$  in Eq. (28):

Here,  $T_0$  and  $N_0$  are temperature and particle number of the hot spot at its stagnation phase, respectively,  $\Delta N = N_0 - N$  is the particle number difference of the hot spot during its expansion phase. On the right-hand side of Eq. (37), the numerator is the total released fusion energy with  $E_{\text{fus}} = 17.6$  MeV, and the denominator is the thermal energy of the hot spot at stagnation phase which approximates to the mechanical work during the compression phase. For the indirect drive laser fusion, to calculate the fusion energy gain  $G$ , one should also consider the absorbed laser efficiency  $\eta_{\text{aL}}$ , the laser-to-X-ray conversion efficiency  $\eta_{\text{LX}}$ , the hohlraum-to-capsule coupling efficiency  $\eta_{\text{HC}}$  and the rocket efficiency  $\eta_{\text{rocket}}$ . Then, the fusion energy gain  $G$  can be written as:

$$G = \eta_{\text{aL}} \eta_{\text{LX}} \eta_{\text{XC}} \eta_{\text{rocket}} G_H. \quad (38)$$

Usually, it requires  $G \geq 1$  for ignition.

Considering a hot spot with initial radius  $R_0 = 0.05$  mm, initial density  $\rho_0 = 75$  g/cm<sup>3</sup>,  $T_0 = 4$  keV and an initial piston velocity  $dR/dt = 0$  at the stagnation, we calculate the expanding dynamics of this hot spot with above simple model. In this calculation, the piston mass includes that of the cool fuel and the remaining ablator, which is set as 10 times of the mass of hot-spot. Presented in Fig. 7 is temporal evolutions of the temperature, the pressure, the released fusion power and  $G$  of the hot-spot with  $\eta_E$  from Eq. (32). For comparison, the hot-spot dynamics calculated with  $\eta_E = \eta_A$  from the AM model [Eq. (1)],  $\eta_E = 1$  (assuming all  $\alpha$ -particles escape out of fuel) and  $\eta_E = 0$  (assuming all  $\alpha$ -particles deposit inside the fuel) are also presented. Here, we take  $\eta_{\text{aL}} \sim 0.85$ ,  $\eta_{\text{LX}} \sim 0.87$ ,  $\eta_{\text{XC}} \sim 0.16$  [7], and  $\eta_{\text{rocket}} \sim 0.17$  [28] in calculating  $G$ . Here, we don't consider the case with  $\eta_E$  from the ZH model, because temperature range of the escape factor expression from this model is limited up to 10 keV, much lower than what we concern for an ignited burning fuel.

As shown in Fig. 7, the  $\alpha$ -particle escape-effect can significantly influence the hot-spot dynamics in burning phase and influence the nuclear energy released by fusion. First, the self-heating effect induced by  $\alpha$ -particles plays a key role in the inertial confinement fusion, which is a prerequisite for ignition. For the case with  $\eta_E = 1$ , i.e., no  $\alpha$ -particle deposition,  $G$  is about zero. Second, the self-heating is significantly connected with the the escape of the  $\alpha$ -particles. At a smaller  $\eta_E$ , i.e., with less  $\alpha$ -particles escaping and so a higher self-heating, the hot spot has a higher temperature, a higher pressure and a higher fusion power. For example, the maximum temperature reaches 63 keV and maximum pressure reaches 1.4 Tbar at

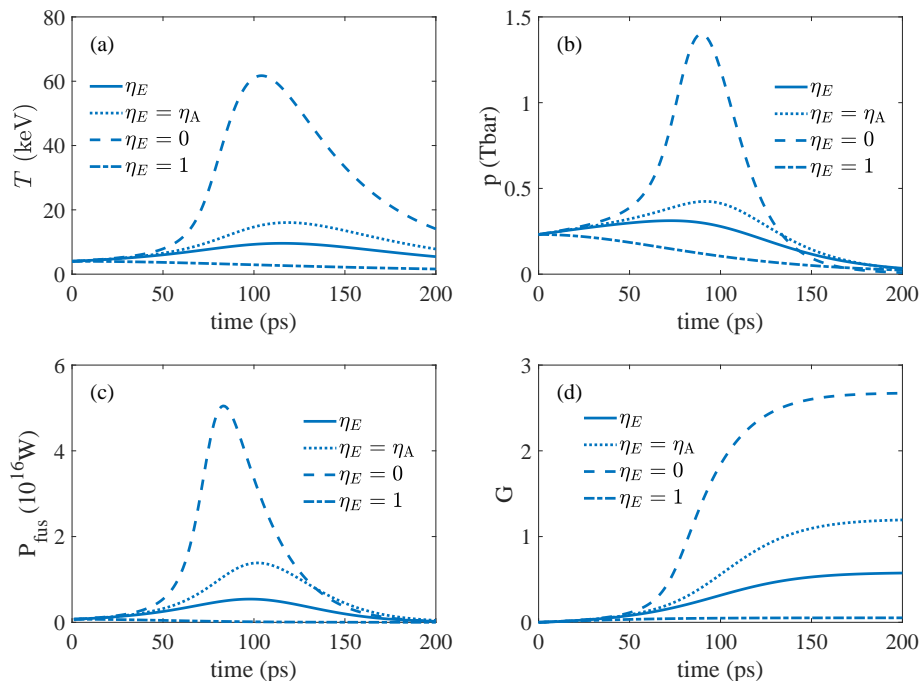


FIG. 7. (Color online) The temporal evolutions of (a) temperature  $T$ , (b) pressure  $p$ , (c) power for nuclear energy releasing  $P_{\text{fus}}$ , and (d) energy gain  $G$  of the hot-spot by using  $\eta_E$  from Eq. (32) (solid line),  $\eta_E = \eta_A$  [Eq. (1)] from the AM model (dotted line),  $\eta_E = 0$  (dashed line) and  $\eta_E = 1$  (dashed dotted line).

$\eta_E = 0$ , while they are only 16 keV and 0.4 Tbar by using  $\eta_E$  from the AM model, and 9 keV and 0.3 Tbar by using  $\eta_E$  from Eq. (32). Thus, it can seriously overestimate the self-heating by assuming all  $\alpha$ -particles are deposited. Third, calculation of the escape factor of  $\alpha$ -particles is important in obtaining a more reliable hot spot dynamics. In contrast to our model by using  $\eta_E$  from Eq. (32), the case with  $\eta_A$  can underestimate the escape-effect, which leads to a higher temperature and a higher pressure of the hot spot. Notice that  $G$  is about 1.2 by using  $\eta_E$  from the AM model, while it is only 0.6 by using  $\eta_E$  from Eq. (32). That is to say, it could ignite by using the AM model, but the ignition fails by using  $\eta_E$  which considers all modifications given in this work. In other words, the escape of  $\alpha$ -particles can remarkably change the ignition condition.

Finally, it is interesting to mention that the  $\alpha$ -particle escape effect can also increase the gain for a violent burning hot-spot with a temperature  $\gtrsim 64$  keV. The reason is that, the reactivity  $\langle\sigma v\rangle$  of the DT fusion decreases with  $T$  at  $T \geq 64$  keV [14] and meanwhile, the escape effect leads to a lower temperature and a lower pressure, and thus a slower expansion and higher density. Because the reaction rate is  $n^2 \langle\sigma v\rangle / 4$ , so the  $\alpha$ -particle escaping from an ignited burning hot-spot with  $\gtrsim 64$  keV can lead to a colder fuel with a larger reactivity and a higher density and thus a higher gain.

## V. SUMMARY

We have studied the  $\alpha$ -particle escape from an burning DT fuel with temperatures up to more than tens keV by consid-

ering modifications of the  $\alpha$ -particle stopping by both DT ions and electrons with their Maxwellian average stopping weights, the relativity effect on electron distribution, and the modified Coulomb logarithm of the DT- $\alpha$  collisions. From our studies, it show that: (1) the deceleration is mainly induced by the electrons for a newborn  $\alpha$ -particle at  $T \leq 50$  keV, while it is fully dominated by the DT ions for a seriously decelerated  $\alpha$  particle or at  $T > 50$  keV; (2) the relativity effect can remarkably decreases the  $\alpha$ -particle stopping by electrons at a high temperature, such as it can decrease by 28% at 100 keV; (3) the modified Coulomb logarithm can be as much as 1.6 times of the ones in AM model. We gave a fitted expression Eq. (32) with consistent geometric treatment, to calculate  $\eta_E$ , which can be applied to the burning plasmas of 1 to 150 keV and 0.04 to 3 g/cm<sup>2</sup> with an accuracy within  $\pm 0.02$ . This expression can be used to estimate the  $\alpha$ -particle escape for a DT fuel with a uniform density and a uniform temperature and with the same temperature for the DT ions and the electrons. However, one should use the integration Eq. (28) to obtain a more reliable escape factor for the hot-spot which plasma status is time and space dependent. We further discussed the  $\alpha$ -particle escape-effect on the hot-spot dynamics by comparing the calculation results with  $\eta_E$  from different models. As a result, the hot-spot dynamics of a burning fuel is strongly connected with the escape of  $\alpha$ -particles. The escape factor of  $\alpha$ -particles from our model is larger than previously published results, which can to a lower self-heating, a lower temperature, a lower pressure, and thus leads to a lower energy gain. The escape of  $\alpha$ -particles may fail the ignition for parameters near the ignition condition. However, for a vio-

lent burning with high temperature ( $\gtrsim 64$  keV), the  $\alpha$ -particle escape can increase the fusion energy gain.

### ACKNOWLEDGMENTS

This work is supported by the China Postdoctoral Science Foundation (under Grant No. 2019M650584).

- 
- [1] J. Nuckolls, L. Wood, A. Thiessen, and G. Zimmerman, *Nature* **239**, 139 (1972).
- [2] K. A. Brueckner and S. Jorna, *Rev. Mod. Phys.* **46**, 325 (1974).
- [3] J. D. Lindl, R. L. McCrory, and E. M. Campbell, *Phys. Today* **45**, 32 (1992).
- [4] E. Campbell, V. Goncharov, T. Sangster, S. Regan, P. Radha, R. Betti, J. Myatt, D. Froula, M. Rosenberg, I. Igumenshchev, W. Seka, A. Solodov, A. Maximov, J. Marozas, T. Collins, D. Turnbull, F. Marshall, A. Shvydky, J. Knauer, R. McCrory, A. Sefkow, M. Hohenberger, P. Michel, T. Chapman, L. Masse, C. Goyon, S. Ross, J. Bates, M. Karasik, J. Oh, J. Weaver, A. Schmitt, K. Obenschain, S. Obenschain, S. Reyes, and B. V. Wotterghem, *Matter and Radiation at Extremes* **2**, 37 (2017).
- [5] S. W. Haan, J. D. Lindl, D. A. Callahan, D. S. Clark, J. D. Salmonson, B. A. Hammel, L. J. Atherton, R. C. Cook, M. J. Edwards, S. Glenzer, A. V. Hamza, S. P. Hatchett, M. C. Herrmann, D. E. Hinkel, D. D. Ho, H. Huang, O. S. Jones, J. Kline, G. Kyrala, O. L. Landen, B. J. MacGowan, M. M. Marinak, D. D. Meyerhofer, J. L. Milovich, K. A. Moreno, E. I. Moses, D. H. Munro, A. Nikroo, R. E. Olson, K. Peterson, S. M. Pol-laine, J. E. Ralph, H. F. Robey, B. K. Spears, P. T. Springer, L. J. Suter, C. A. Thomas, R. P. Town, R. Vesey, S. V. Weber, H. L. Wilkens, and D. C. Wilson, *Physics of Plasmas* **18**, 051001 (2011).
- [6] K. Lan, J. Liu, D. Lai, W. Zheng, and X.-T. He, *Phys. Plasmas* **21**, 010704 (2014); K. Lan, X.-T. He, J. Liu, W. Zheng, and D. Lai, *Phys. Plasmas* **21**, 052704 (2014); K. Lan and W. Zheng, *Phys. Plasmas* **21**, 090704 (2014).
- [7] K. Lan, J. Liu, Z. Li, X. Xie, W. Huo, Y. Chen, G. Ren, C. Zheng, D. Yang, S. Li, Z. Yang, L. Guo, S. Li, M. Zhang, X. Han, C. Zhai, L. Hou, Y. Li, K. Deng, Z. Yuan, X. Zhan, F. Wang, G. Yuan, H. Zhang, B. Jiang, L. Huang, W. Zhang, K. Du, R. Zhao, P. Li, W. Wang, J. Su, X. Deng, D. Hu, W. Zhou, H. Jia, Y. Ding, W. Zheng, and X. He, *Matter and Radiation at Extremes* **1**, 8 (2016).
- [8] W. Y. Huo, Z. Li, Y.-H. Chen, X. Xie, G. Ren, H. Cao, S. Li, K. Lan, J. Liu, Y. Li, S. Li, L. Guo, Y. Liu, D. Yang, X. Jiang, L. Hou, H. Du, X. Peng, T. Xu, C. Li, X. Zhan, Z. Wang, K. Deng, Q. Wang, B. Deng, F. Wang, J. Yang, S. Liu, S. Jiang, G. Yuan, H. Zhang, B. Jiang, W. Zhang, Q. Gu, Z. He, K. Du, X. Deng, W. Zhou, L. Wang, X. Huang, Y. Wang, D. Hu, K. Zheng, Q. Zhu, and Y. Ding, *Phys. Rev. Lett.* **120**, 165001 (2018).
- [9] W. M. Manheimer, D. G. Colombant, and J. H. Gardner, *Phys. Fluids* **25**, 1644 (1982).
- [10] M. Murakami and K. Nishihara, *Jpn. J. App. Phys.* **26**, 1132 (1987).
- [11] J. D. Lindl, *Inertial Confinement Fusion* (Springer-Verlag, 1998) Chap. 5.
- [12] O. N. Krokhin and V. B. Rozanov, *Sov. J. Quantum Electron.* **2**, 393 (1973).
- [13] G. S. Fraley, E. J. Linnebur, R. J. Mason, and R. L. Morse, *Phys. Fluids* **17**, 474 (1974).
- [14] S. Atzeni and J. Meyer-ter Vehn, *The Physics of Inertial Fusion* (Oxford University Press, 2004).
- [15] A. B. Zylstra and O. A. Hurricane, *Phys. Plasmas* **26**, 062701 (2019).
- [16] X. Ribeyre, V. T. Tikhonchuk, J. Breil, M. Lafon, and E. L. Bel, *Phys. Plasmas* **18**, 102702 (2011).
- [17] H.-S. Park, O. Hurricane, D. Callahan, D. Casey, E. Dewald, T. Dittrich, T. Döppner, D. Hinkel, L. B. Hopkins, S. L. Pape, T. Ma, P. Patel, B. Remington, H. Robey, J. Salmonson, and J. Kline, *Phys. Rev. Lett.* **112** (2014).
- [18] O. A. Hurricane, D. A. Callahan, D. T. Casey, P. M. Celliers, C. Cerjan, E. L. Dewald, T. R. Dittrich, T. Döppner, D. E. Hinkel, L. F. B. Hopkins, J. L. Kline, S. L. Pape, T. Ma, A. G. MacPhee, J. L. Milovich, A. Pak, H.-S. Park, P. K. Patel, B. A. Remington, J. D. Salmonson, P. T. Springer, and R. Tommasini, *Nature* **506**, 343 (2014).
- [19] B. Cheng, T. J. T. Kwan, Y. M. Wang, F. E. Merrill, C. J. Cerjan, and S. H. Batha, *Phys. Plasmas* **22**, 082704 (2015).
- [20] O. A. Hurricane, D. A. Callahan, D. T. Casey, E. L. Dewald, T. R. Dittrich, T. Döppner, S. Haan, D. E. Hinkel, L. F. B. Hopkins, O. Jones, A. L. Kritcher, S. L. Pape, T. Ma, A. G. MacPhee, J. L. Milovich, J. Moody, A. Pak, H.-S. Park, P. K. Patel, J. E. Ralph, H. F. Robey, J. S. Ross, J. D. Salmonson, B. K. Spears, P. T. Springer, R. Tommasini, F. Albert, L. R. Benedetti, R. Bionta, E. Bond, D. K. Bradley, J. Caggiano, P. M. Celliers, C. Cerjan, J. A. Church, R. Dylla-Spears, D. Edgell, M. J. Edwards, D. Fittinghoff, M. A. B. Garcia, A. Hamza, R. Hatarik, H. Herrmann, M. Hohenberger, D. Hoover, J. L. Kline, G. Kyrala, B. Koziolowski, G. Grim, J. E. Field, J. Frenje, N. Izumi, M. G. Johnson, S. F. Khan, J. Knauer, T. Kohut, O. Landen, F. Merrill, P. Michel, A. Moore, S. R. Nagel, A. Nikroo, T. Parham, R. R. Rygg, D. Sayre, M. Schneider, D. Shaughnessy, D. Strozzi, R. P. J. Town, D. Turnbull, P. Volegov, A. Wan, K. Widmann, C. Wilde, and C. Yeamans, *Nat. Phys.* **12**, 800 (2016).
- [21] C.-K. Huang, K. Molvig, B. J. Albright, E. S. Dodd, E. L. Vold, G. Kagan, and N. M. Hoffman, *Phys. Plasmas* **24**, 022704 (2017).
- [22] B. Cheng, T. J. T. Kwan, S. A. Yi, O. L. Landen, Y. M. Wang, C. J. Cerjan, S. H. Batha, and F. J. Wysocki, *Phys. Rev. E* **98** (2018).
- [23] T. J. M. Boyd and J. J. Sanderson, *The Physics of Plasmas* (Cambridge University Press, 2003) p. 8.
- [24] F. Jüttner, *Ann. Phys.* **339**, 856 (1911).
- [25] M. Abramowitz and I. A. Stegun, eds., *Handbook of Mathematical Functions with Formulas, Graphs, and Mathematical Tables*, Vol. 56 (United States Department Of Commerce, 1972) p. 375.
- [26] J. Wesson, *Tokamaks* (Oxford University Press, 2004).

[27] L. M. Hively, *Nucl. Technol./Fusion* **3**, 199 (1983).

[28] J. Lindl, *Phys. Plasmas* **2**, 3933 (1995).